Polarization compensating protective coatings for TPF-Coronagraph optics to control contrast degrading cross polarization leakage

Kunjithapatham Balasubramanian*, Daniel J. Hoppe, Pantazis Z. Mouroulis, Luis F. Marchen, and Stuart B. Shaklan
Jet Propulsion Laboratory, California Institute of Technology
4800 Oak Grove Drive, Mail Stop: 301-451, Pasadena, CA 91109.

ABSTRACT

The Terrestrial Planet Finder Coronagraph (TPF-C) for observing and characterizing exo-solar planets requiring star light suppression to 10^{-10} level demands optical aberrations and instrument stability to sub-nm levels. Additionally, wavefront polarization has to be tightly controlled over the 8m x 3.5m primary mirror aperture and 500nm – 800nm minimum bandwidth because the Deformable Mirror (DM) employed to control the wavefront can not correct simultaneously for the different wavefronts presented by two orthogonal uncorrected polarization fields. Further, leakage of cross polarization fields introduced by the various optical surfaces can degrade the image contrast. The study reported here shows mirror coating designs that reduce the phase difference between orthogonal polarizations reflected by a mirror surface to less than 0.6 deg over the bandwidth and aperture which may encounter a maximum angle of incidence of about 12 deg at a curved mirror. Such designs mitigate the contrast degradation due to cross polarization leakage. Simulations show that required contrast levels can be achieved with such coatings.

Keywords: Terrestrial Planet Finder Coronagraph, coatings, polarization, wavefront, exo-solar, planet, contrast

1. INTRODUCTION

Controlling the phase difference between orthogonal polarization fields reflected by mirrors at non normal incidence, (particularly curved mirrors, for example primary and secondary mirrors of a telescope), is necessary for some applications such as the TPF Coronagraph (TPF-C)[1],[2] which also demands very stringent requirements on uniformity of amplitude and phase of reflected light from the telescope mirrors. Cross polarization leakage has to be controlled to achieve the performance specifications and error budget[3] of TPF-C. The phase difference between x and y polarizations of the light that reaches the coronagraph from the main optical telescope assembly (OTA) of the system consisting of 20 or more mirror surfaces (curved as well as plane mirrors) should be minimized close to zero. Conventionally, aluminum and silver mirrors are employed in space and ground based telescope mirrors particularly when the science interests are in the visible spectrum. Both types of mirrors require protective overcoats to prevent performance degradation due to oxidation and other effects over the life of the mirrors or mission. Typically a dielectric layer, for example of MgF_2 or of SiO_x (x denoting a chosen stoichiometry of the oxide), is coated on aluminum and silver mirrors respectively. Layers of other compounds such as HfO_2, Si_3N_4 and Al_2O_3 could also be employed. When reflected phase has to be controlled in addition to environmental protection, the overcoat layer/layers have to be chosen and designed to achieve the required performance over the wavelength band. We describe here the design approaches and performance analysis of the OTA in the wavelength band of interest. Coronagraph performance at 600nm wavelength based on a particular coating and occulting focal plane mask is also presented.

2. SILVER VS. ALUMINUM MIRRORS FOR TPF-C

TPF Coronagraph optics should have high reflectivity over the full bandwidth of interest to the mission, i.e., from 500nm to 800 nm as a minimum and desirably up to 1100 nm. Aluminum and silver are candidate materials for the mirrors. General issues on the choice of telescope mirror materials, deposition and performance have been discussed in the

* Email : kbala@jpl.nasa.gov, Phone: 818-393-0258, Fax: 818-393-4950

literature[4]. Reflectivity vs. wavelength of common mirror materials is compared in Figure 1 based on optical constants data from Essential Macleod[5] extended materials database which are similar to those found in Palik[6] for metals. While the UV reflectivity of Al is attractive for science interests in the UV region, the dip around 800nm presents a severe reduction in throughput particularly when several surfaces are considered. Reflectivity of evaporated metal films typically show higher reflectivity than bulk polished metals (Hass and Hadley)[7]. Employing optical constants of evaporated films of silver and aluminum from Hass and Hadley (also of Essential Macleod Standard materials database), Figures 2 and 3 compare the reflected throughput which suffers significantly even with only 4 reflections when Al is employed. With simple protective coatings with minimal effect on polarization, the throughput suffers even more with Al. Figures 4 and 5 compare Rp/Rs and delta phase between reflected polarizations for the two metals from 0 to 15 deg angle of incidence (AOI). Simple protective coatings show that silver performs better than aluminum for throughput as well as polarization and hence, silver is currently the material of choice for TPF-C optics.

3. TYPICAL PROTECTIVE COATINGS FOR SILVER MIRRORS

Silver is soft and also suffers from tarnishing typically due to chemical reaction with sulfur containing vapors and hence requires an effective protective coating considering the many years the mirrors will spend on ground before launch into space. Jacobson et al[4] studied silver coating options for Gemini 8-m telescope. Common commercial silver mirrors may have a half wave thick SiO_x or Al_2O_3 protective layer to prevent chemical attack over time. However, for specific polarization performance over wavelength and angle of incidence, the protective coating needs careful optimization. TPF-C primary and secondary mirrors are large and manufacturing constraints demand that the layers be of simple structure so that uniformity of reflectivity can indeed be achieved with available coating technology base. Besides assuring environmental protection, an ideal protective coating should provide high reflectivity in the wavelength region of interest and over the entire aperture i.e., uniform reflectivity over all angles of incidence. Secondly, the coating should minimize polarization effects; i.e., the two orthogonal polarizations should have nearly equal amplitude and phase on reflection over all relevant angles of incidence (AOI) and wavelengths.

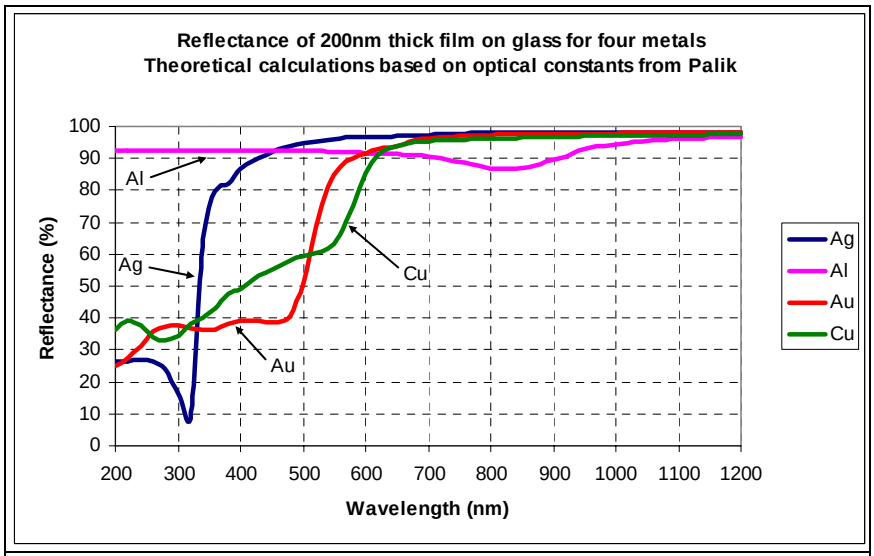

Figure 1. Reflectance of common mirror metals at normal incidence

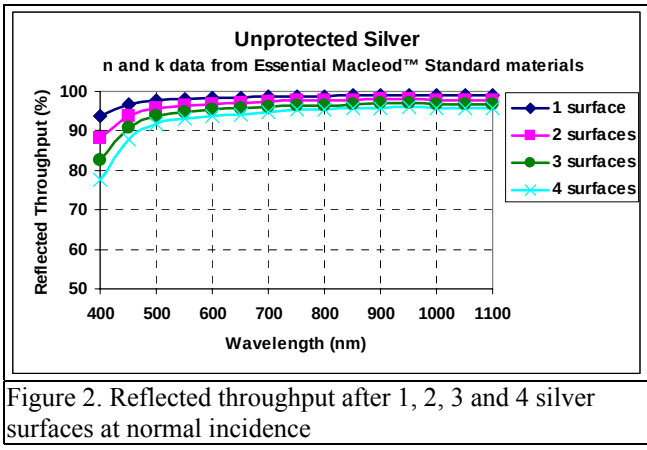

Figure 2. Reflected throughput after 1, 2, 3 and 4 silver surfaces at normal incidence

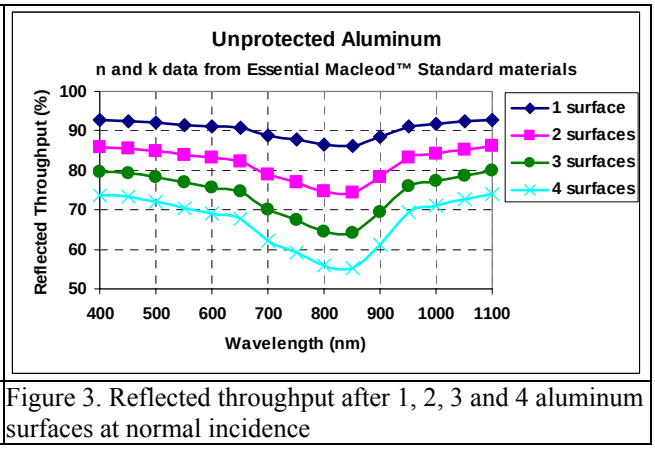

Figure 3. Reflected throughput after 1, 2, 3 and 4 aluminum surfaces at normal incidence

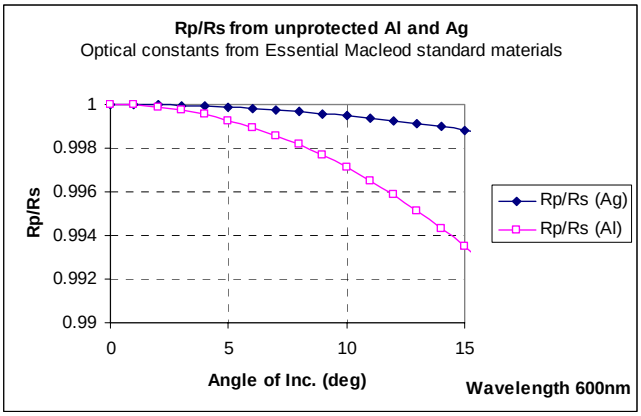

Figure 4. Rp/Rs vs. Angle of Incidence

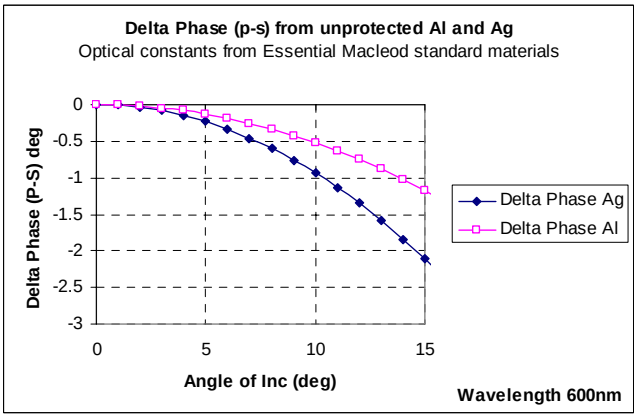

Figure 5. Delta phase (p-s) vs. Angle of Incidence

4. A SIMPLE PROTECTIVE COATING ON SILVER TO OPTIMIZE POLARIZATION PHASE DIFFERENCE

In order to reduce the phase difference between orthogonal polarizations p and s, on refection from a silver mirror, a simple coating of SiO_2 can be applied as a protective layer. Applying one layer of a well characterized material in terms of fabrication process ensures less uncertainties in the practical manufacture of such a mirror, even though the uniformity requirements of TPF Coronagraph requires us to study the process and the resulting coatings more carefully than ever before. Figures 6a and 6b show the reflectivity and delta phase (phase difference between p and s polarizations on reflection) of unprotected silver. A simple half wave thick SiO_2 coating (~ 205nm thick) on silver may protect it for common applications; however the polarization performance is not optimum for TPF-C, though reflectivity is >98% from 550 to 1050nm. Figure 7a and 7b show the reflectivity and delta phase for such a mirror. Figure 8a and 8b show the same for 124nm thick SiO_2 protected silver. The maximum angle of incidence encountered by any ray in the telescope primary or secondary mirror is about 12 deg. These figures were generated with optical constants data from Essential Macleod Standard materials database which are similar to those from Hass and Hadley[5] for evaporated films. Both the reflectivity difference and delta phase between p and s polarizations are minimized in this case within the bandwidth of interest. Note that the phase difference delta is maximum at 600nm for this design by choice. A small change in the thickness of the overcoat will alter the peak location in the band without seriously affecting the overall performance. Manufacturing variances in optical constants and thickness of the layers could cause such shifts and hence this design should be taken as a conceptual guideline. For example, keeping the optical constants the same and changing the thickness of the SiO_2 layer by 10nm to 134nm shifts the peak within the band to 650nm without significantly altering the general shape of the curves. It should be noted that 2π excursions in the phase have been removed for clarity in the plots.

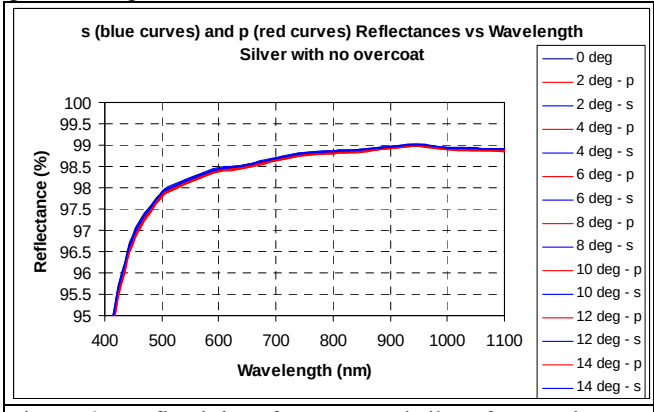

Figure 6a. Reflectivity of unprotected silver for p and s polarizations for angles of incidence 2 to 14 deg in steps of 2 deg.

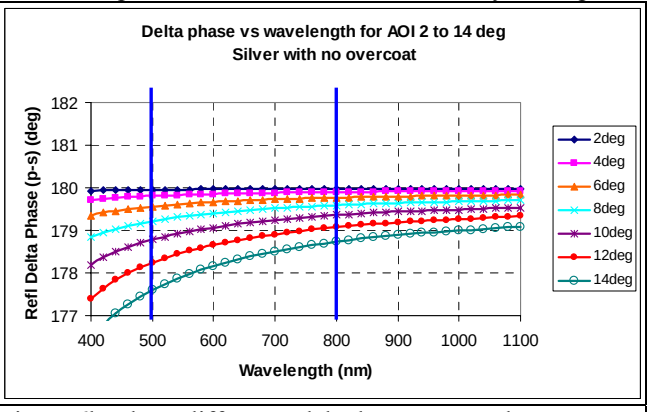

Figure 6b. Phase difference delta between p and s polarizations for unprotected silver at angles of incidence 2 to 14 deg in steps of 2 deg.

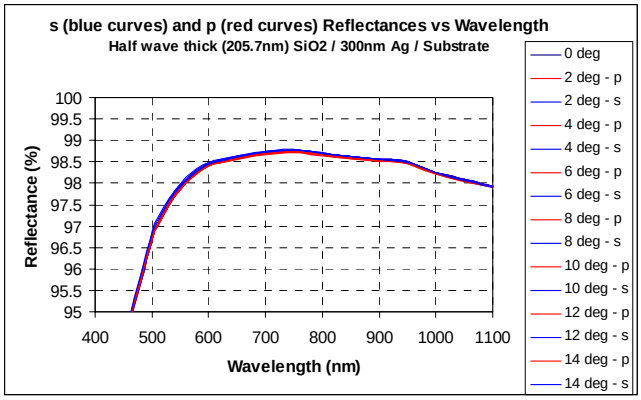

Figure 7a. Reflectivity of silver mirror protected with half wave thick (205.7nm) SiO_2 layer; p and s polarizations for angles of incidence 0 to 14 deg in steps of 2°

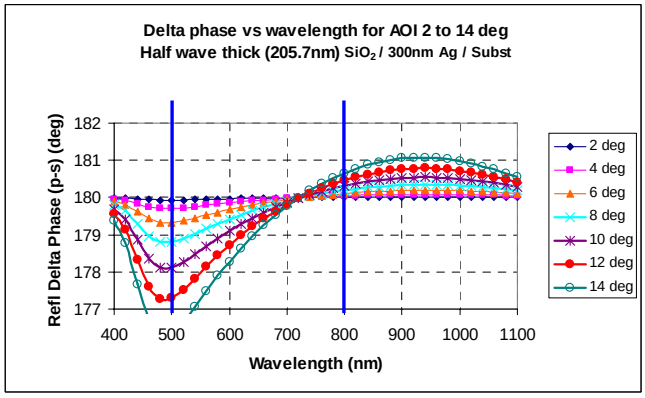

Figure 7b. Phase difference delta between p and s polarizations for silver mirror protected with half wave thick (205.7nm) of SiO_2 layer; angles of incidence 0 to 14 deg in steps of 2°

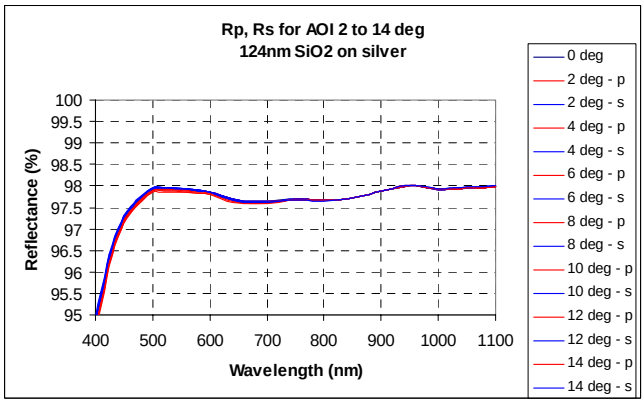

Figure 8a. Reflectivity of silver mirror protected with 124nm of SiO_2 layer; p and s polarizations for angles of incidence 0 to 14 deg in steps of 2°

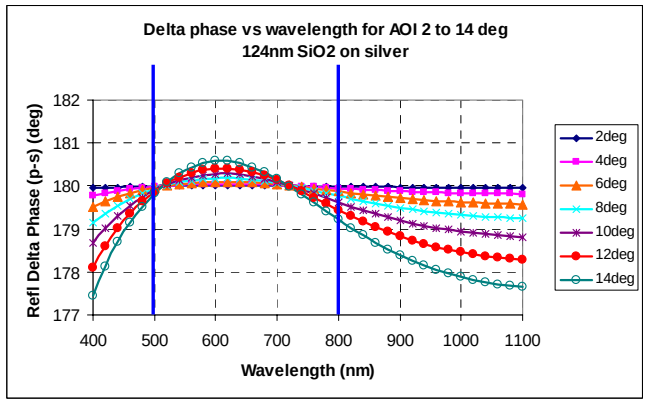

Figure 8b. Phase difference delta between p and s polarizations for silver mirror protected with 124nm of SiO_2 layer; angles of incidence 0 to 14 deg in steps of 2°

5. ALTERNATE DESIGNS

An effective overcoat has to satisfy other practical requirements such as good adhesion and low stress, besides meeting reflectivity and polarization requirements. Wolfe et al [8] have studied alternate coating designs with excellent protection as well as UV enhancement of reflectance. In order to minimize stress, one may have to apply additional thin layers between the substrate and the protective coatings. A possible approach may be to use a thin layer of Si_3N_4 on either side of the SiO_2 layer, which may also provide adequate environmental protection, though to be experimentally verified. While the particular thickness will depend on experimental results that confirm minimum stress and excellent protection, a potential design is suggested as shown with calculated results in Figure 9. Small variations in thickness will alter the location of the minimum phase difference within the band without significantly affecting the over all behavior. The optical constants depend critically on the process parameters and hence such a reference design could be taken as a guide for detailed experimental work. Such a design also offers the potential for wider bandwidth, though the outer angles show larger than desirable delta.

Another potential design approach involves coatings that compensate the polarization effects induced by one mirror with the opposite effect induced by another. For example, the primary and secondary mirrors could have different coatings in

such a way that the net effect on the field after reflection from both mirrors will be minimum. An example of such a design approach and resulting reflectance and phase difference between p and s are illustrated in Figures 10 and 11.

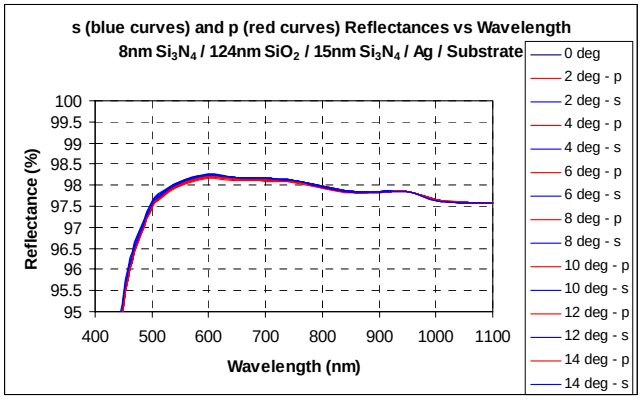

Figure 9a. Reflectivity of silver mirror coated with 8nm Si_3N_4/124nm SiO_2/15nm Si_3N_4/300nm Ag layers

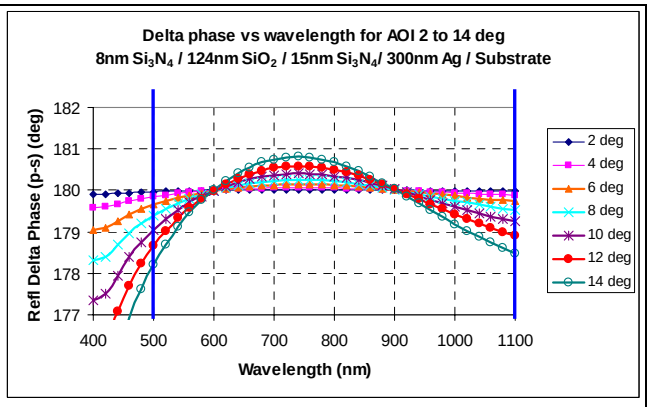

Figure 9b. Delta phase (p-s) of silver mirror coated with 8nm Si_3N_4/124nm SiO_2/15nm Si_3N_4/300nm Ag layers

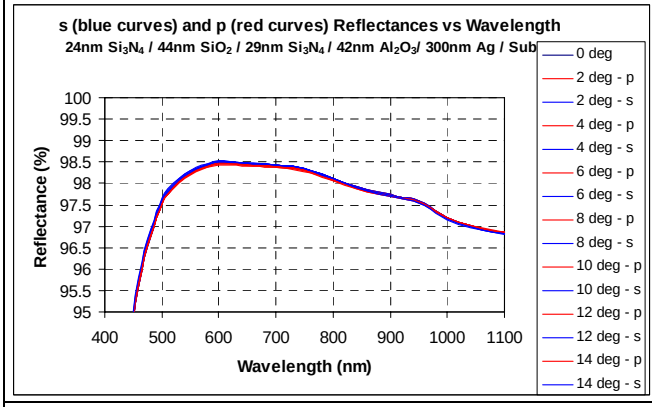

Figure 10a. Reflectivity of silver mirror coated with 24nm Si_3N_4/44nm SiO_2/29nm Si_3N_4/42nm Al_2O_3/300nm Ag layers

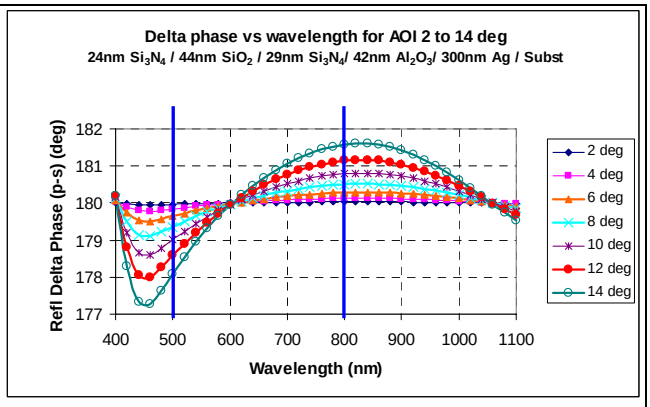

Figure 10b. Delta phase (p-s) of silver mirror coated with 24nm Si_3N_4/44nm SiO_2/29nm Si_3N_4/42nm Al_2O_3/300nm Ag layers

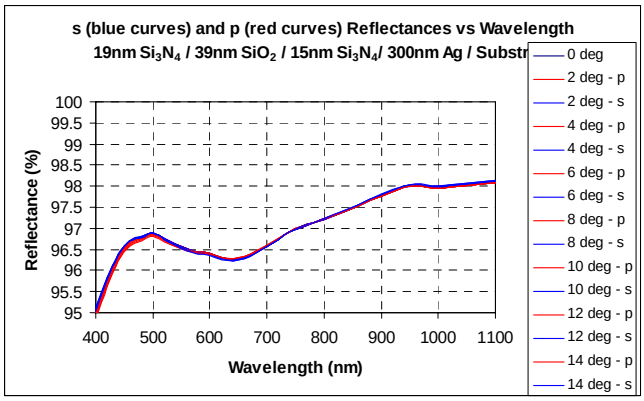

Figure 11a. Reflectivity of silver mirror coated with 19nm Si_3N_4/ 39nm SiO_2/15nm Si_3N_4/300nm Ag layers

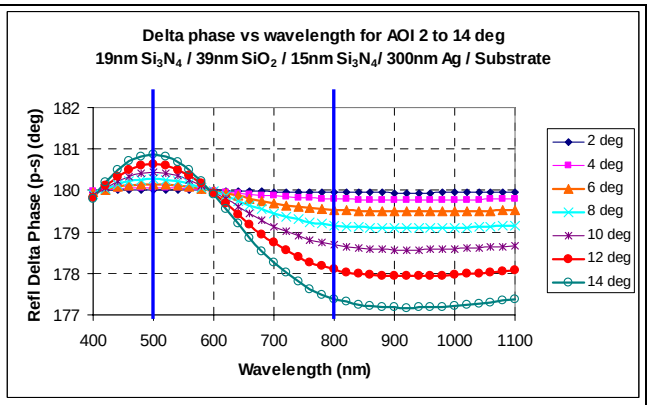

Figure 11b. Delta phase (p-s) of silver mirror coated with 19nm Si_3N_4/ 39nm SiO_2/15nm Si_3N_4/300nm Ag layers

Note that the polarities of the phase difference delta are complementary between primary and secondary mirrors potentially canceling each other, if not perfectly. We have not yet examined the propagation of a ray from the entrance

aperture to the image plane with such coatings and hence the effectiveness of such an approach has not yet been established. Also, the throughput which is also very important for the total system performance may suffer with such a design, though it is not necessary to apply such a coating to all the mirrors in the system.

Due to the large mirror size (8m x 3.5m elliptical primary being the candidate for TPF-C) and deposition process constraints, multilayer coatings are a challenge to achieve the required uniformity in thickness and refractive of index of these layers together with stress balance and environmental protection. Therefore, the current preferred choice for TPF-C mirrors is a single layer overcoat with required thin adhesion and stress balancing layers as suggested in Figures 8 and 9.

6. BASELINE OPTICAL DESIGN OF TPF-C OTA

Current baseline design[9] of TPF Coronagraph employs an 8x3.5m elliptical shape off-axis primary mirror and a 0.88x0.38m secondary mirror separated by 12m and with an effective focal length of 140m. The maximum angle of incidence encountered by any ray at the primary or secondary is less than 12 deg. Figure 12 shows the schematic of the current baseline design of TPF-Coronagraph up to a polarizing beam splitter which splits the light into two paths, designed so for treating two orthogonal polarizations separately as well as for assuring redundancy in the system. Optimized coatings that minimize or eliminate polarization effects and thus meet contrast requirements may offer the potential for simplifying the system design by avoiding two independent coronagraph paths.

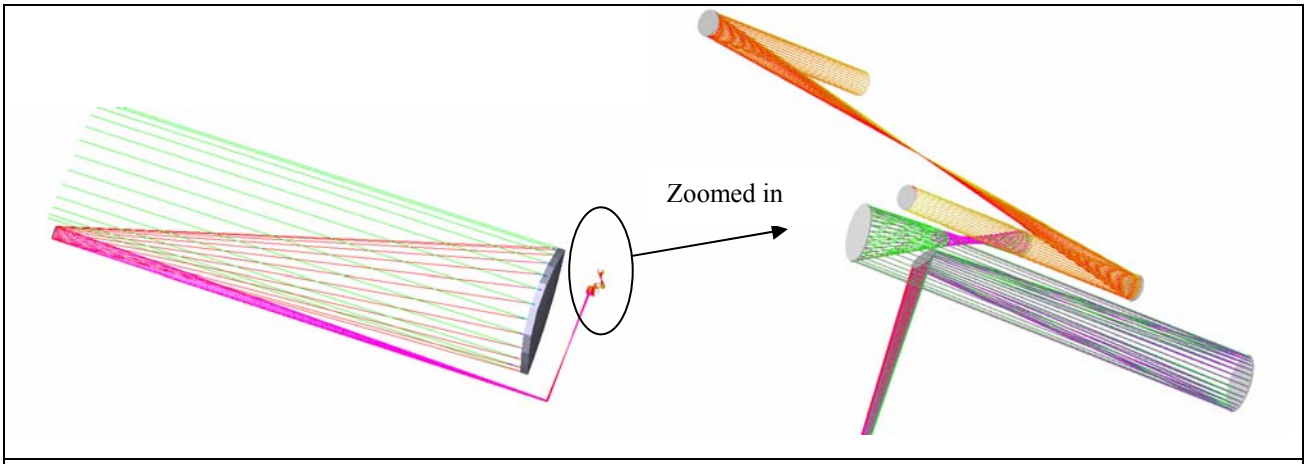

Figure 12. Schematic of the baseline TPF-Coronagraph optics up to the polarizing beam splitter that separates the two polarizations into two parallel coronagraph arms.

7. POLARIZATION FIELDS EXTRACTED AT A PLANE NEAR THE PUPIL BEFORE THE CORONAGRAPH OCCULTING MASK

Employing a Zemax macro developed[10] for the purpose, the complex polarized fields are extracted at a plane before the polarizing beam splitter in the system. These fields are then analyzed to assess the influence of cross polarization terms on the contrast achievable through the coronagraph. Figure 13 shows the conceptual approach to the analysis of the coronagraph system.

The total field at the pupil can be described as follows.

$$\text{Total Field} = A_{xx}e^{i\phi_{xx}} + a_{xy}e^{i\phi_{xy}} + A_{yy}e^{i\phi_{yy}} + a_{yx}e^{i\phi_{yx}}$$

where “A” refers to the main term and “a” refers to the cross term induced in the system due to various reflections. The subscripts xx refer to the x polarization field at the pupil after all the mirrors for the x field incident at the entrance aperture. The subscripts xy refer to the x field created by incident y field and similarly yx refers to the y field created by incident x field.

If we consider the first two terms that will pass through the "x" arm of the coronagraph, a residual field will remain uncorrected after the Deformable Mirror (DM). This uncorrected residual field will degrade the contrast at the image plane.

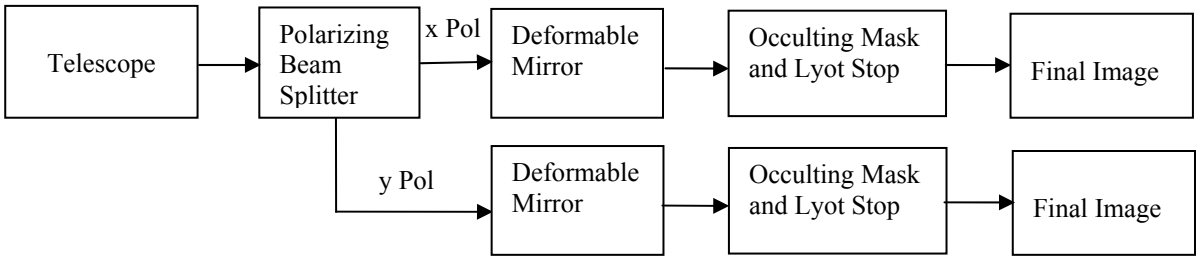

Figure 13. Simple schematic of the coronagraph simulation

8. CROSS TERMS INFLUENCING THE CONTRAST

The field after perfect correction of the main term at the DM in the x arm of the coronagraph can be written as,

$$1 + \left(\frac{a_{xy}}{A_{xx}} \right) e^{i(\phi_{xy} - \phi_{xx})}$$

where a_{xy}/A_{xx} represents the amplitude perturbation due to the cross polarization term and $\phi_{xy} - \phi_{xx}$ represents the phase perturbation in an otherwise ideally corrected field. The same would be the case for the y polarization arm of the coronagraph. These leakage terms degrade the contrast achievable with the coronagraph. In the following sections, we show an example illustrating the effectiveness of optimum coating to achieve the desired contrast.

9. DIFFRACTION ANALYSIS OF CONTRAST

In this section we describe results from a simple coronagraph model employing diffraction analysis of complex fields including amplitude and phase, and compare results for optimum and non optimum mirror coatings. The model consists of a pupil plane, occulting mask plane, Lyot plane, and final image plane, (Figure 14). Ideal imaging is assumed through a set of ideal lenses placed as in figure 14 and therefore propagation from one plane to the next is effectively a Fourier transform (FFT) of the complex fields. In all cases, an ideal occulting mask and Lyot stop are assumed. The wavelength of the simulation is fixed at 600 nm; a 100 mm diameter pupil and F/60 optics are assumed. Figure 15 describes the band-limited 1-Sinc^2 occulting mask used in the model.

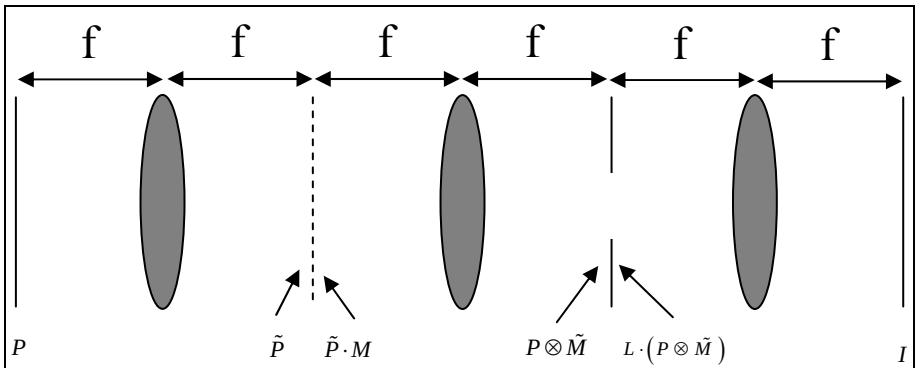

Figure 14. Coronagraph diffraction model (P=Pupil Field, M=Mask, L=Lyot Stop, I=Final Image, ~ Indicates Fourier Transform).

We also assume that there are corrective optics, for example a pair of deformable mirrors, that may be adjusted to correct one of four field profiles in the pupil to the ideal pupil field consisting of uniform amplitude and phase, (Figure 16). As

described in section 7, the four possible pupil fields are E_{xx}, the x-polarized pupil field for x-polarization incident on the telescope, E_{yx}, the y-polarized pupil field for x-polarization incident on the telescope, and the counterparts for y-polarization incident, E_{yy}, and E_{xy}. The coating design strives to eliminate the cross-polarized fields, E_{xy} and E_{yx}, and equalize the co-polarized fields E_{xx} and E_{yy}. If this ideal situation can be achieved then a single setting of the corrective optics will produce ideal pupil plane fields for both incident polarizations. Of course the ideal case is never achieved, and in this section we report the contrast achievable for the three other components when one is corrected, for the cases of optimum and non-optimum mirror coatings.

The next several figures present field profiles at various points in the coronagraph for one particular choice of pupil plane field and setting of the corrective optics. Similar calculations were performed for all cases of interest and are summarized later in tabular form. Figure 17 shows the pupil plane field for the cross polarized field E_{xy} when the corrective optics are adjusted to optimize the E_{xx} field. As shown in the figure 17a, the field in the pupil has a maximum amplitude of approximately $5x10^{-3}$, or an intensity of $25x10^{-6}$.

The figure also shows that the phase varies considerably across the pupil. The corresponding Lyot plane fields are shown in Figure 18. Here we see that before masking by the stop, the field is concentrated near the edges of the re-imaged pupil, as expected. Due to the non-uniform amplitude and phase of the original pupil field there is a residual field after passing through the eye-shaped stop. This field is in turn responsible for a non-zero field in the final image plane.

The final contrast for this case is shown in Figure 19. Contrast is defined as the leakage of the on-axis field at each point in the final image plane relative to the field incident from that particular location. Thus the contrast is affected by both the leaked field and the throughput of a mask at a given location. Since the occulting mask has zero throughput for X=0 the contrast is undefined there, resulting in the red stripe in the plot in Figure 19b. For field locations significantly larger than approximately 4λ/D the mask throughput is nearly unity and the contrast plot is very nearly equal to the leakage of the on-axis source.

For fields sufficiently removed from X=0 the figure shows that the first-order contrast requirement for TPF-C of a contrast better than 10^{-10} is met. In order to compare results for a number of cases we define two regions in the final image plane for average and worst-case contrast calculations. These regions are depicted in Figure 19b. The first is a square region of size λ/D, centered at X=4λ/D, Y=0. The second, larger, region extends from X=4λ/D to 14λ/D, and Y=-10λ/D to +10λ/D. Computed contrast values for 600nm wavelength within these boxed regions when a linear 1-sinc^2 mask is employed, are tabulated for various main and cross polarization fields. In all cases, the contrast values are in acceptable range for the optimum coating if we assume that all other aberrations are negligible or correctable.

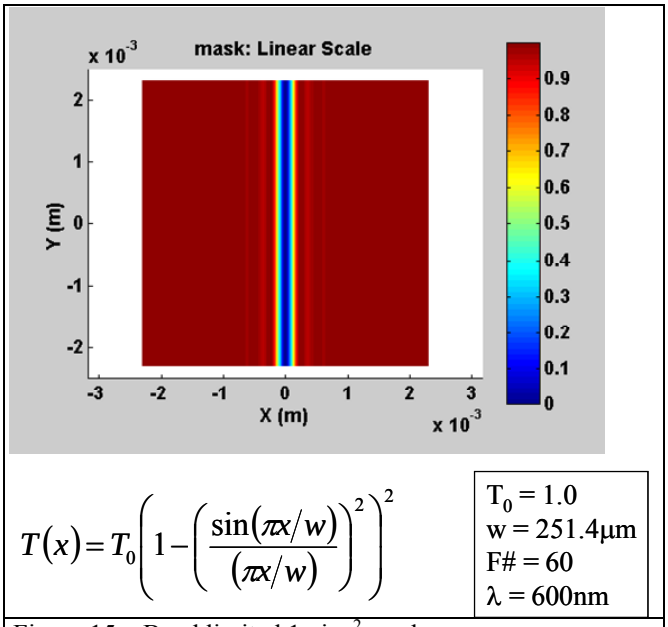

Figure 15. Band limited 1-sinc^2 mask.

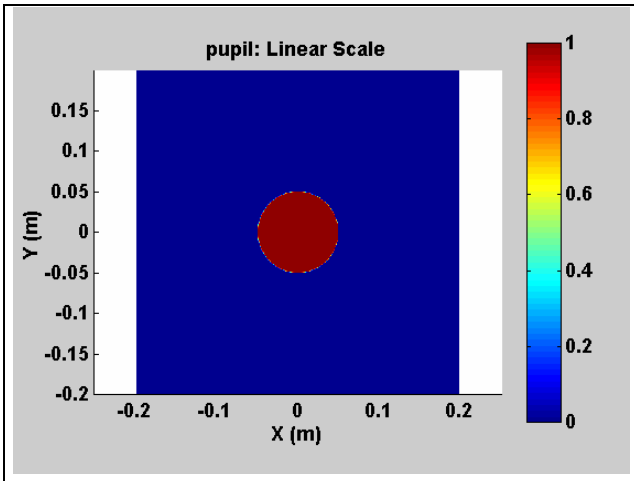

Figure 16. Ideal (uniform) 100mm dia pupil plane field.

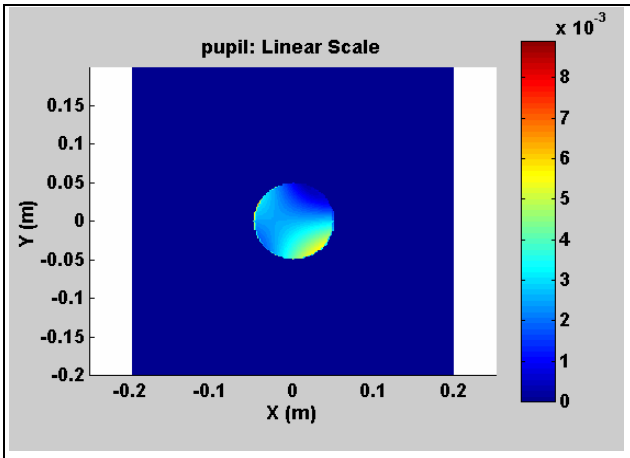

Figure 17a. An example of cross polarized field. Amplitude of E_{xy} normalized to co-polarized field

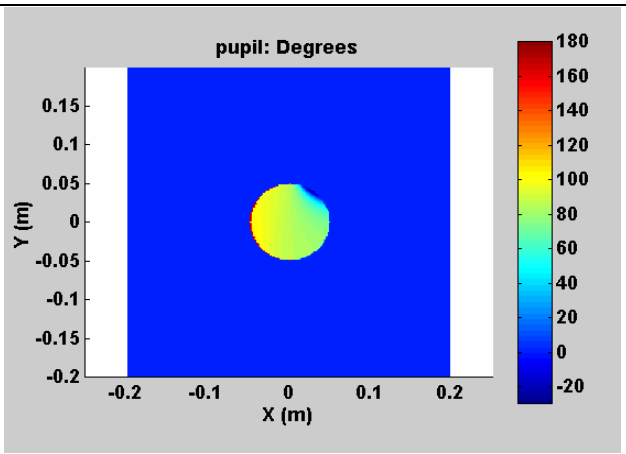

Figure 17b. An example of cross polarized field. Phase of E_{xy} normalized to co-polarized field

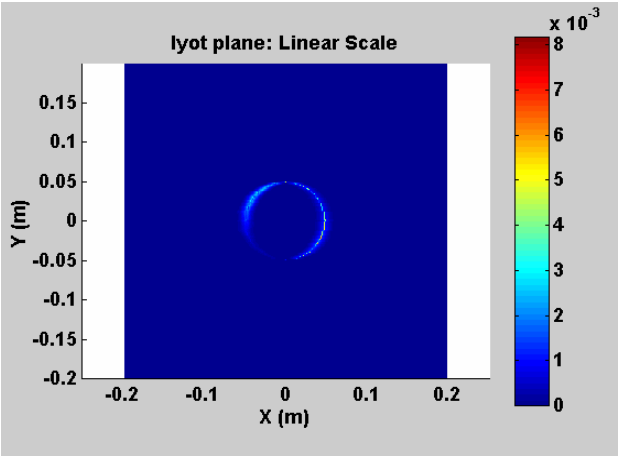

Figure 18a. Amplitude of cross polarization term E_{xy}/E_{xx} of figure 17 at the Lyot Plane before Lyot stop

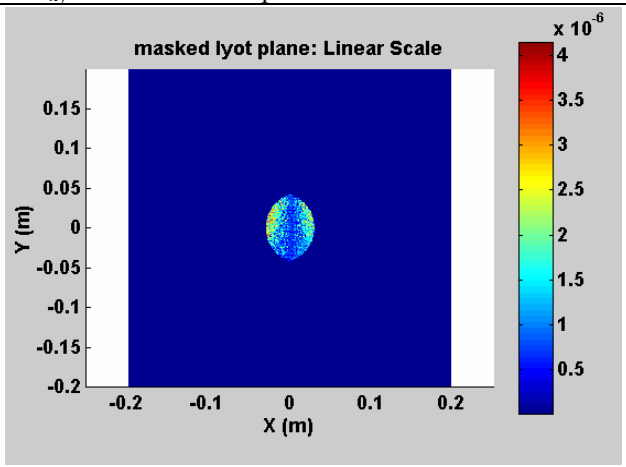

Figure 18b. Amplitude of cross polarization term E_{xy}/E_{xx} of figure 17 after an eye shaped Lyot stop (100mm dia open circles with 30 mm center to center spacing)

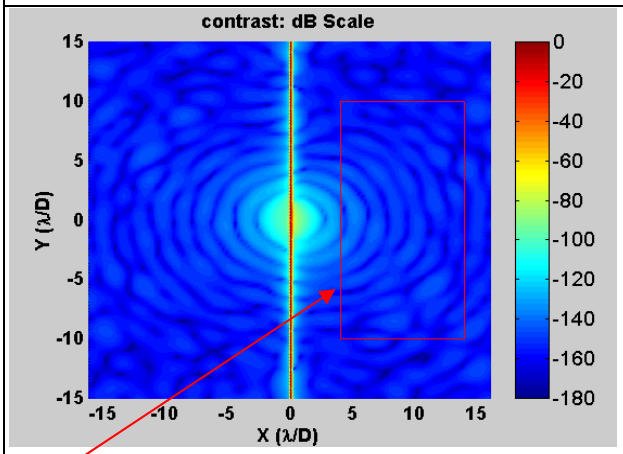

Rectangular box region from 4 to 14 λ/D in x and -10 to +10 λ/D in y

Figure 19a. Contrast at image plane for cross polarization field E_{xy} shown in figure 17

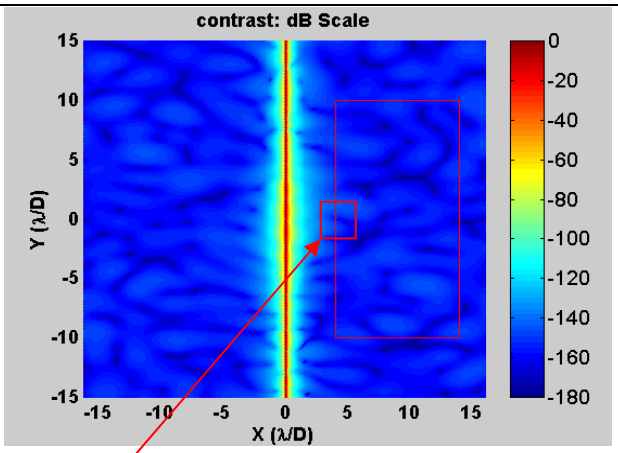

Square box region from 3.5 to 4.5 λ/D in x and -0.5 to +0.5 λ/D in y

Figure 19b. Contrast definition boxes (an example)

Pupil Field	Average Contrast (λ/D 3.5-4.5)	Worst Contrast (λ/D 3.5-4.5)	Average Contrast (λ/D 4-14)	Worst Contrast (λ/D 4-14)
YY/XX (1/2-Wave Coating)	5.9E-10	9.9E-10	4.5E-11	9.9E-10
XY/XX (1/2-Wave Coating)	7.8E-13	2.3E-12	3.8E-14	7.2E-13
YX/XX (1/2-Wave Coating)	8.9E-12	1.6E-11	1.2E-12	1.3E-11
XX/YY (1/2-Wave Coating)	5.6E-10	9.9E-10	4.6E-11	9.9E-10
XY/YY (1/2-Wave Coating)	9.9E-13	2.9E-12	5.0E-14	1.0E-12
YX/YY (1/2-Wave Coating)	1.1E-11	2.2E-11	1.2E-12	1.2E-11
YY/XX (Optimized Coating)	7.7E-11	1.2E-10	5.3E-12	1.2E-10
XY/XX (Optimized Coating)	2.2E-14	6.5E-14	1.2E-15	2.4E-14
YX/XX (Optimized Coating)	4.2E-14	1.3E-13	2.2E-15	6.5E-14
XX/YY (Optimized Coating)	7.4E-11	1.2E-10	5.4E-12	1.2E-10
XY/YY (Optimized Coating)	2.0E-14	5.8E-14	9.5E-16	1.9E-14
YX/YY (Optimized Coating)	4.0E-14	1.2E-13	2.0E-15	6.5E-14
Ideal (Uniform)	6.1E-18	9.2E-18	1.1E-18	1.8E-17

Table 1. Contrast for various pupil fields

Table 1 above summarizes the contrast results for a number of cases of interest. Maximum and average contrast values, in each of the two regions, is shown for half wave protective coating, optimized coating (124nm SiO_2 on silver), and the ideal pupil case. For each of the coating cases six entries are given, corresponding to the three remaining polarizations assuming the corrective optics are set to correct either the E_{xx} or E_{yy} field. The ideal pupil case is included to illustrate the numerical noise floor of the computation which is in the 10^{-17}-10^{-18} range. The table shows that the worst contrast results are for the opposite polarization, that is E_{yy} when the correction is set for E_{xx}, or vice-versa, and is $\sim 10^{-10}$ for the optimized coating case whereas the same field shows a contrast of $\sim 10^{-9}$ for the non-optimum coating case. The cross-polarized fields are significantly lower in all cases, approaching 10^{-13} or better. Figure 20 compares the contrast for the two coatings for the various pupil fields as in Table 1. While the above analysis is for one wavelength in the middle of the band of interest, we continue to study the behavior of the system with various coating options for other wavelengths to ensure optimum performance over the full bandwidth of interest.

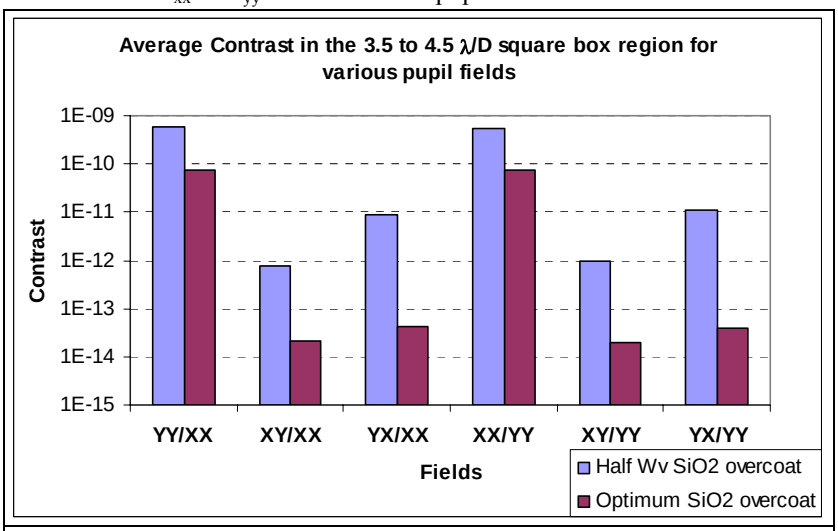

Figure 20. Contrasts for various normalized pupil fields; calculations are based on full field diffraction models through the coronagraph. Two coatings are compared. 1) all silver mirrors over-coated with 124nm of SiO_2 and 2) all silver mirrors over-coated with half wave thick (205nm) SiO_2; the calculations are done for 600nm wavelength.

The 8th order mask proposed by Kuchner et al[11] and further studied by Shaklan and Green[13] show less contrast sensitivity to aberrations[12,13] compared to the 1-sinc^2 mask, easing the polarization performance requirements of coatings and allowing for much needed tolerance margins. Our preliminary analysis pending detailed studies with the 8th order mask indicates such an improvement.

10. CONCLUSIONS

Protective coatings on silver mirrors can be designed to minimize cross polarization leakage into the TPF coronagraph. Example designs with simple layer structures are illustrated as a guideline. Contrast calculations based on diffraction analysis at one wavelength suggest that with a linear 1-sinc^2 occulting mask one can meet coronagraph contrast requirements assuming other aberrations will be minimized in the system. Cross polarization leakage terms get significantly reduced with such designs. Broadband performance is under evaluation. Preliminary studies with 8th order occulting mask suggest that polarization contribution to contrast will be much reduced. Practical realization depends on coating process technology in the large scale required for the primary and secondary mirrors. Further work on broad band performance will lead to guidelines for manufacturing tolerance requirements. A more detailed publication on the diffraction modeling including broad band model is planned for the future.

11. ACKNOWLEDGEMENTS

The authors acknowledge the valuable discussions with Chuck Bowers of Goddard Space Flight Center, Maryland. Leonard Wayne of JPL developed the Zemax macros needed for extracting polarization fields at various planes in the coronagraph system. This work was performed at the Jet Propulsion Laboratory, California Institute of Technology, under a contract with the National Aeronautics and Space Administration. Reference herein to any specific commercial product, process or service by trade name, trademark, manufacturer, or otherwise, does not constitute or imply its endorsement by the United States Government or the Jet Propulsion Laboratory, California Institute of Technology.

12. REFERENCES

[1] Breckinridge, J. B. and Ben R. Oppenheimer, "Polarization effects in reflecting coronagraphs for white-light applications in astronomy", ApJ 600, pp.1091-1098, Jan 2004

[2] Elias II, Nicholas M., R. Bates, J. Turner-Valle, "Polarization analysis of Terrestrial Planet Finder coronagraph designs" in Instruments, Methods and Missions for Astrobiology VIII, Ed. Richard B. Hoover, Gilbert V. Levin, Alexie V. Rozanov, Proc SPIE Vol. 5555, pp. 248-257, 2004.

[3] Stuart B. Shaklan, L.F. Marchen, and J. J. Green, , "The Terrestrial Planet Finder Coronagraph error budget" in Techniques and Instrumentation for Detection of Exoplanets II, Ed. Daniel R. Coulter, Proc SPIE Vol 5905, 2005.

[4] Jacobson, M. R., et al., "Development of silver coatings options for the Gemini 8-M telescopes Project", in Advanced Technology Optical/IR Telescopes VI, Ed. Larry M. Stepp, Proc SPIE Vol. 3352, pp. 477-502, 1998.

[5] Essential Macleod – an optical thin film design software from Thin Film Center, Inc., Tucson, AZ, USA

[6] Edward Palik, Handbook of Optical Constants of Solids, Academic Press, 1998, 1995, pages 285, 291-295, 355-357, 396-399.

[7] Hass, G and L. Hadley, Optical constants of metals, in American Institute of Physics Handbook, D.E. Gray, Editor. 1972, McGraw Hill Book Company: New York and London. p. 6.124-6.156.

[8] Jesse Wolfe, David Sanders, Steve Bryan, and Norman Thomas, "Deposition of durable wideband silver mirror coatings using long-throw, low-pressure, DC-pulsed magnetron sputtering", in Specialized Optical Developments in Astronomy, Ed. Eli Atad-Ettedgui and Sandro D'Odorico, Proc. SPIE Vol. 4842, pp. 343-351, 2003.

[9] Pantazis Z. Mouroulis and S. B. Shaklan, presentation at the SPIE Optics & Photonics Symposium Conference 5874, San Diego CA 2-4 August 2005, "Optical Design of the Terrestrial Planet Finder Coronagraph" in Current Developments in Lens Design and Optical Engineering VI, Proc. SPIE Vol. 5874, 2005.

[10] Leonard Wayne of JPL developed the Zemax macro needed to extract polarization fields at any surface in the optical telescope assembly of the coronagraph

[11] Kuchner, M. J., J. Crepp and J. Ge, "Eighth-Order Image Masks for Terrestrial Planet Finding", submitted to ApJ in Nov 2004.

[12] Green, J.J. and S. B. Shaklan, Optimizing coronagraph designs to minimize their contrast sensitivity to low-order optical aberrations, in Techniques and Instrumentation for Detection of Exoplanets, Ed. Daniel R. Coulter, Proc. SPIE Vol. 5170, pp 25-37, 2003.

[13] Shaklan, S. B. and J. J. Green, "Low-Order Aberration Sensitivity of Eighth-Order Coronagraph Mask," ApJ, Accepted 2005.